



An augmented seismic network to study off-shore seismicity around the Maltese Islands: The FASTMIT experiment

G. Bozionelos^{*1}, P. Galea¹, S. D'Amico¹, M. P. Plasencia Linares², M. Romanelli², G. Rossi², S. Parolai², A. Vuan², M. Sugan², M. R. Agius¹

¹Department of Geosciences, University of Malta, Msida, Malta

²Seismological Research Department - CRS, National Institute of Oceanography and Applied Geophysics - OGS, Italy.

Abstract. Appropriate planning and deployment of a seismic network is a prerequisite to efficiently monitor seismic activity, determine the seismic source, and eventually contribute to the seismotectonic interpretation and seismic hazard assessment. The evaluation and effectiveness of a local network on the Maltese islands, recently extended by a further six seismic stations for one year, is presented. We investigate the new temporary network's data and site selection quality, utilizing spectral patterns in the seismic data and also evaluate the network's event location performance by relocating a number of recorded events. The results will be significant for the future installation of permanent seismic stations on the Maltese islands.

Acknowledgements. We would like to thank all the people who helped in the installation of the stations, especially the personnel of Mдина's Natural History Museum, Heritage Malta (Haġar Qim temples), Bird Park Malta (near St Michael's chapel), the curator of St Michael chapel Father Christian Borg, Prof. Raymond Ellul and Mr Martin Saliba from the University of Malta, Gozo Campus, Mr Joe Pace who kindly provided his farmhouse in Siġġiewi, Father Raymond Francalanza and Marvic Gauci for providing a room and help at Bahrija Church.

1 Introduction

The Maltese islands (figure 1) have been affected by several earthquakes in the historical past. The epicentres of these earthquakes were located mainly in the Sicily Channel (bordered by the Sicilian, Tunisian, and Libyan coastlines), in eastern Sicily, and as far away as the Hel-

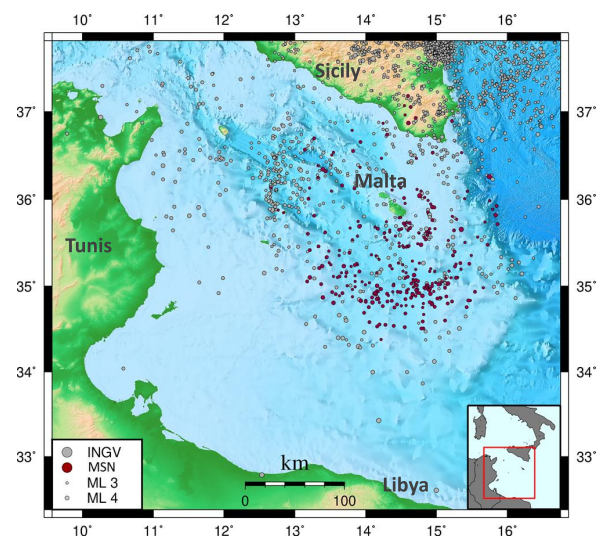


Figure 1: Seismicity in the Sicily Channel for the period 1995 – 28 November 2018. Epicentres from INGV (grey dots); Malta Seismic Network (MSN) single station (pre-2014) and MSN most reliable locations for events greater than ML 2.5 (red dots) for the period 1995 until 28 November 2018. Many events appear to be located south of Malta, being focused on the local major tectonic fault zones.

*Correspondence to: G. Bozionelos (georgebozionelos@gmail.com)

lenic arc. Contrary to the common belief that Malta is not at risk from earthquakes, some of these events produced considerable damage to local buildings (Galea, 2007). The main damaging events were located in Sicily (1542 M_w 6.6, I_{max} VII on Malta; 1693, M_w 7.4 I_{max} on Malta VII–VIII; 1911 I_{max} Malta VII), Crete (1856, M_w 7.7, I_{max} Malta VII), Ionian (1743, M_w 6.9, I_{max} Malta VII) and Aegean Sea (1886 M_w 7.3, I_{max} Malta VI–VII), where the intensities are on the EMS-98 scale. The risk from seismic hazard is increasing because of the rapid expansion of the construction industry, still not regulated by a national building code.

Because of the unique position of the Maltese Islands in the Mediterranean Sea, and to achieve better earthquake detection in the region, different types of seismographs were installed in Malta since the introduction of seismographic instrumentation at the beginning of the 20th century. A Milne horizontal pendulum seismograph operated in Valletta from 1906 until the 1950s. A vertical long-period Sprengnether seismograph with photographic recording was installed in 1977, operating for some years and then replaced by a three-component short period station with analogue paper recording. The seismograms from these instruments are still preserved by the Seismic Monitoring and Research Group within the Department of Geosciences at the University of Malta, and many of them have been scanned within the SISMOS project (<http://sismos.rm.ingv.it>). Since June 1995 and until 2014, only one broadband station was operating in Malta at Wied Dalam (Agius et al., 2014). WDD was installed as part of the MedNet program (Boschi et al., 1994). Since 2015, the Malta Seismic Network was set up, initially consisting of only three stations (Agius et al., 2015).

WDD seismic station is located in the south-eastern part of the island, housed in a disused tunnel at a distance of about 900 meters from the coast (figure 2A). WDD is located on Lower Coralline limestone, the oldest of the four main geological formations outcropping on the Maltese archipelago (figure 2B). The isolated installation and quiet environment allow high-quality low noise recordings. It was thus possible to achieve the detection of several local and regional events (Agius et al., 2011) (figure 1). Many of these events occurring close to Malta were too small to be detected by other regional operating stations, and they may have been misclassified or overlooked due to low signal-to-noise ratio. Although the single station location algorithm provides reasonable epicentres, it is unable to determine the depth of the earthquakes, and also suffers from limited accuracy and low precision solutions, especially when the signal-to-noise ratio at the P-onset is low. The significant number of events being detected by the single station, however, highlighted the need to improve earthquake

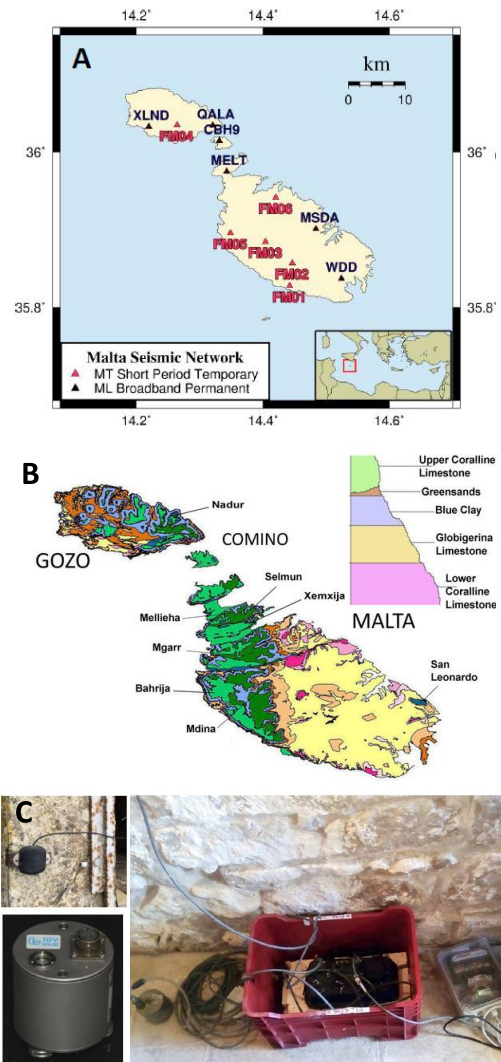


Figure 2: A: The enhanced seismic network. The stations are depicted with red triangles for the six short period OGS stations and with black triangles for the six permanent stations of Malta Seismic Network. B: Geological map of the Maltese Islands after Pedley et al. (1976). C: Typical station setup for the enhanced network experiment, here station FM02 inside the farmhouse at Siggiewi. Top right frame: The GPS receiver placed outside the site. Bottom left frame: The Lennartz seismometer. Right frame: The case holding the data logger.

locations and detectability. Enhancement of the observational capacity was essential for improving the accuracy and precision of the hypocentral solutions, and for identifying active faults in and around the Maltese islands. The Malta Seismic Network was thus established and extended in recent years and currently comprises six permanent broadband stations installed across the Maltese islands (figure 2A, black triangles). The improved detectability (Galea et al., 2018) and the number of the events being obtained by the new network (figure 1), encouraged us to further extend it, and 6 short period temporary stations were installed from June 2017 and operated until September 2018, improving the coverage of the network for more than a year (figure 2A, red triangles). This extension allowed the exploration of the potentials of installing more permanent stations and also helped to test the installation sites. This paper describes the temporary extended network, and evaluates the station quality and performance, focussing on the six temporary stations.

2 The FASTMIT Project

The FASTMIT project (Rossi et al., 2016) was funded by the Italian government and coordinated by the OGS (*Istituto Nazionale di Oceanografia e di Geofisica Sperimentale, Sezione Centro Ricerche Sismologiche, Italy*). The main FASTMIT goals are to study the offshore seismicity in the Italian seas as well as in adjacent ones. This is necessary in order to increase the scientific knowledge related to fault systems at sea and their evolution in a broader geodynamic context. Recent studies and observations have highlighted the presence of potential seismogenic and tsunamigenic areas in the Central Mediterranean region, which are not yet well understood and are not fully integrated with seismic and tsunami hazard evaluations (Petricca et al., 2019). During the project, four areas have been investigated (Adriatic Sea, the Taranto Gulf, the Sicily Channel, and the southern Tyrrhenian Sea). In particular, studies have focussed on the improvement of seismic hazard analysis, coastal hazards with a focus on areas in which critical infrastructures are present, or for the evaluation of the hazard associated with off-shore hydrocarbon extraction operations. FASTMIT benefited from numerous other previous and simultaneous research projects and initiatives (e.g., RITMARE, EMODnet–Geology2, EPOS IP, ASTARTE, SHARE, AlpArray). The team consisted of over 60 researchers which provided a pool of different expertise to tackle all the problems related to the mapping and study of the off-shore seismogenic and tsunamigenic structures. Seismic, chirp, and multibeam surveys provided a better definition of the sea bottom and of the tectonic structures beneath it. Moreover, the cross-border (Italy, Austria, Slovenia, Croatia) seismic net-

work CE3RN (Bragato et al., 2014) was strengthened. The temporary array installed in Malta had the main goal to create an international research framework operational even after the end of the project, and more importantly to test and increase the seismic detection capability in the Central Mediterranean and supply useful information to permanent inland networks which, due to their geometry, suffer from a lack of resolution and accuracy both in terms of earthquake location and magnitude threshold in this region.

3 New Enhanced Network

From June 2017 to September 2018, in the framework of the FASTMIT project, six short-period stations, equipped with Lennartz sensors and RefTek digitizers, were installed across the Maltese archipelago (figure 2A) and integrated with the permanent Malta Seismic Network. FASTMIT stations were operating offline and data acquisition along with maintenance checks were carried out through frequent visits to the stations. Four of the six stations (FM01, FM02, FM04, FM06) were installed directly on the Globigerina or Lower Coralline limestone. These are the two lower outcropping compact formations lying below the soft and erodible Blue Clay (Farrugia et al., 2016; Pedley et al., 1976). Two other stations, FM03, and FM05, were installed on the Upper Coralline Limestone formation. This compact Upper Coralline limestone represents the youngest formation of the Maltese geological sequence and lies above the Blue Clay formation. Its position, above the Blue Clay, makes Upper Coralline limestone not ideal for seismic station installation, as site amplification (as described further below, figure 8) and alteration in the frequency content of seismic waves is consistently observed (Farrugia et al., 2016). Nevertheless, the installation of these stations was considered useful as a means to evaluate quantitatively, and in more detail, within future studies, the influence of the clay layer on the seismic site response to incoming earthquake waves due to this particular geological setting. Table 1 contains a summary related to the installation of each station. The installation took into account noise levels and the security of the operating conditions. Locations as far away as possible from anthropogenic sources of noise were preferred. Being on a small island, it is in general, challenging to avoid noise from anthropogenic and industrial sources, as well as marine-generated noise from nearby coasts. Nevertheless, sheltered locations offering constant power supply and security for the stations were sought.

4 Performance Evaluation

4.1 Initial Waveform Inspection

An initial visual inspection of the 24-hour seismogram plots was first carried out to ensure the proper function-

Station Code	Latitude (°N)	Longitude (°E)	Elevation (m)	Location	Sensor	Digitizer	Outcropping Geology
FM01	35.8276	14.4426	128	Haġar Qim temples	Lennartz	RefTek	Lower Coralline Limestone
FM02	35.8569	14.4467	95	Sigġiewi farmhouse	Lennartz	RefTek	Globigerina Limestone
FM03	35.8845	14.4043	190	Mdina – Natural History Museum	Lennartz	RefTek	Upper Coralline Limestone
FM04	36.0342	14.2647	105	University of Malta, Gozo Campus	Lennartz	RefTek	Globigerina limestone
FM05	35.8959	14.3492	205	Baħrija Church - St Martin of Tours	Lennartz	RefTek	Upper Coralline Limestone
FM06	35.9411	14.4208	6	San Mikiel Chapel, Burmarrad	Lennartz	RefTek	Lower Coralline Limestone
WDD	35.8373	14.5242	44	Wied Dalam, Birżebbuġa	STS-2	Quanterra	Lower Coralline Limestone
MSDA	35.9012	14.4840	48	University of Malta, Msida Campus	Trillium 120PA	Centaur	Globigerina Limestone
MELT	35.9750	14.3430	98	St Agata Tower, Mellieħa	Trillium 120PA	Centaur	Upper Coralline Limestone
QALA	36.0339	14.3210	92	Qala, Chapel of Immaculate Conception, Gozo	Trillium Compact	Centaur	Upper Coralline Limestone
CBH9	36.0140	14.3314	28	Comino, Borehole 9	Trillium Compact	Centaur	Upper Coralline Limestone
XLND	36.0323	14.2199	15	Underground Flour Mill, Xlendi, Gozo	Trillium Compact	Centaur	Lower Coralline Limestone

Table 1: Summary of the stations installed during the experiment (FMXX) and MSN permanent stations

ing of a station. [Figure 3](#) shows 24h plots for the day in which the network recorded one of the largest regional offshore events of the study period. The ML 3.1 event occurred on the 23rd of November, 2017, at 08:36 UTC, about 50 km SW of Malta, and is marked with a yellow star in [figure 3](#). As shown in the figure, stations FM01 (Haġar Qim), FM05 (Baħrija), and FM06 (Salini) are characterised by a lower noise level on this day, making the recording of this event clearer. On the contrary, FM03 (Mdina), FM04 (University of Malta, Gozo Campus), and FM02 (Siggiewi) appear very noisy during that day. On all the 24h plots, the noise is reduced dramatically during the night, indicating the relationship of the noise with human activity. The highest noise levels are recorded at FM03 in Mdina. Although it is known that light industrial activity was going on close to the station during the day, the noise here continues into the night-time hours, indicating that it may not be all anthropogenic. This effect is probably related mainly to two factors. Firstly, the clay subsurface layer (which, in Mdina, is found only 9 m below the base of the Upper Coralline Limestone, has been observed to cause significant amplification and frequency content alternations (Farrugia et al., 2016)). Secondly, the high noise may be attributed to Mdina's geomorphology. Mdina, being built on a hill, is more exposed to bursts of strong wind during the winter months. The noise at FM04 station, installed within the University of Malta, Gozo campus at Xewkija, on the Upper Globigerina limestone, is most likely related to nearby traffic, maintenance works and farming activity that took place during the station's operating period. Any new station at this site would preferably be located instead on the Middle Globigerina limestone in the basement level of the campus, which is presently being rehabilitated. Noise at FM02 (Siggiewi) is also likely to be related to local anthropogenic activity, such as farming. At both stations FM04 and FM03, the primary source of noise is very close, mainly agricultural activities taking place in the adjacent field for FM04 (approx. 10 m away) and renovation activities taking place at the building hosting FM03. Nevertheless, during periods when presumably human activity is low, the stations performed well, as it will be shown in the following sections. Low noise levels at FM01 and FM06 are probably because the stations are sited on the compact Lower Coralline Limestone and in quiet areas.

4.2 Seismic Noise Analysis

Probabilistic Power Spectral Density (PPSD) plots are here utilized to assess the operation and the ambient noise levels that are recorded at the stations ([figures 4 and 9 to 15](#)). The PPSDs are obtained following the approach of McNamara et al. (2004), implemented in the software package ObsPy (Beyreuther et al., 2010), which was used for this study. Following the default

method that it is incorporated in the algorithm, PSSDs are computed by analysing continuous traces of recordings in 1 hour windows that move in steps of 30 minutes. Pre-processing of the 1-hour segments includes segmentation into 13 windows that overlap by 75%, truncation to the next lower power of 2, and subtraction of the mean and tapering. After the removal of instrument response, fast Fourier transform (FFT) is applied to all data segments, and PSDs are obtained from the FFT components. Histograms showing the frequency distributions of the amplitudes recorded at each period based on all smoothed PSDs are created. A probability density function is estimated from the histogram for each centre period. The periods are converted to frequencies, so the final plots of PPSDs show the amplitudes most frequently observed at each frequency. An example of PPSD analysis is given in [figure 4](#), in which plots were created for all stations for the one-week period 11-19 May 2018. Above approximately 0.2 Hz, the PPSDs for all stations lie within the new high and low noise model (NHNM-NLNM) of Peterson (1993), demonstrating high performance. At the stations FM01 and FM05, PPSDs appear to touch the NHNM close to 1 Hz. In the case of FM01, this may be due to energetic wave action at the nearby shore, while for FM05, this could be related to the underlying geological conditions, however it needs further investigation. To further examine the performance of the stations, PPSD plots were created for the entire period of the experiment for all the FASTMIT stations ([figure 9](#)). Since the sensors are short-period, only the 0.5-60 Hz frequency interval is relevant. The performance seems to be satisfactory for all the stations, with all the PPSD plots generally lying within the high and low noise model (NHNM-HLNM, marked with thick lines on the plot) of Peterson (1993). The only exception is station FM05 where exceedance of the NHNM is partly observed between 0.7 and 3.5 Hz. PPSD curves for FM01 are slightly exceeding the NHNM between 0.6 to 1.5 Hz. This is probably due to the station being located close to the cliff and the sea wave activity. In addition, this exceedance may be linked with the location of the sensor. In spite of the ideal conditions of the site (Lower Coralline limestone and away from human noise sources), the seismometer had to be obligatorily placed on a tiled floor. Moreover, close to the end of the experiment, it was discovered that an irrigation pipe was passing underground, close, and below the instrument. In general, all stations show similar noise frequency characteristics, with a broad peak around 0.5 Hz. FM05 consistently demonstrates a smaller peak at around 5 Hz, which is observable on all subsequent plots.

To investigate the effect of the weather conditions, separate PPSD plots are created for the winter and sum-

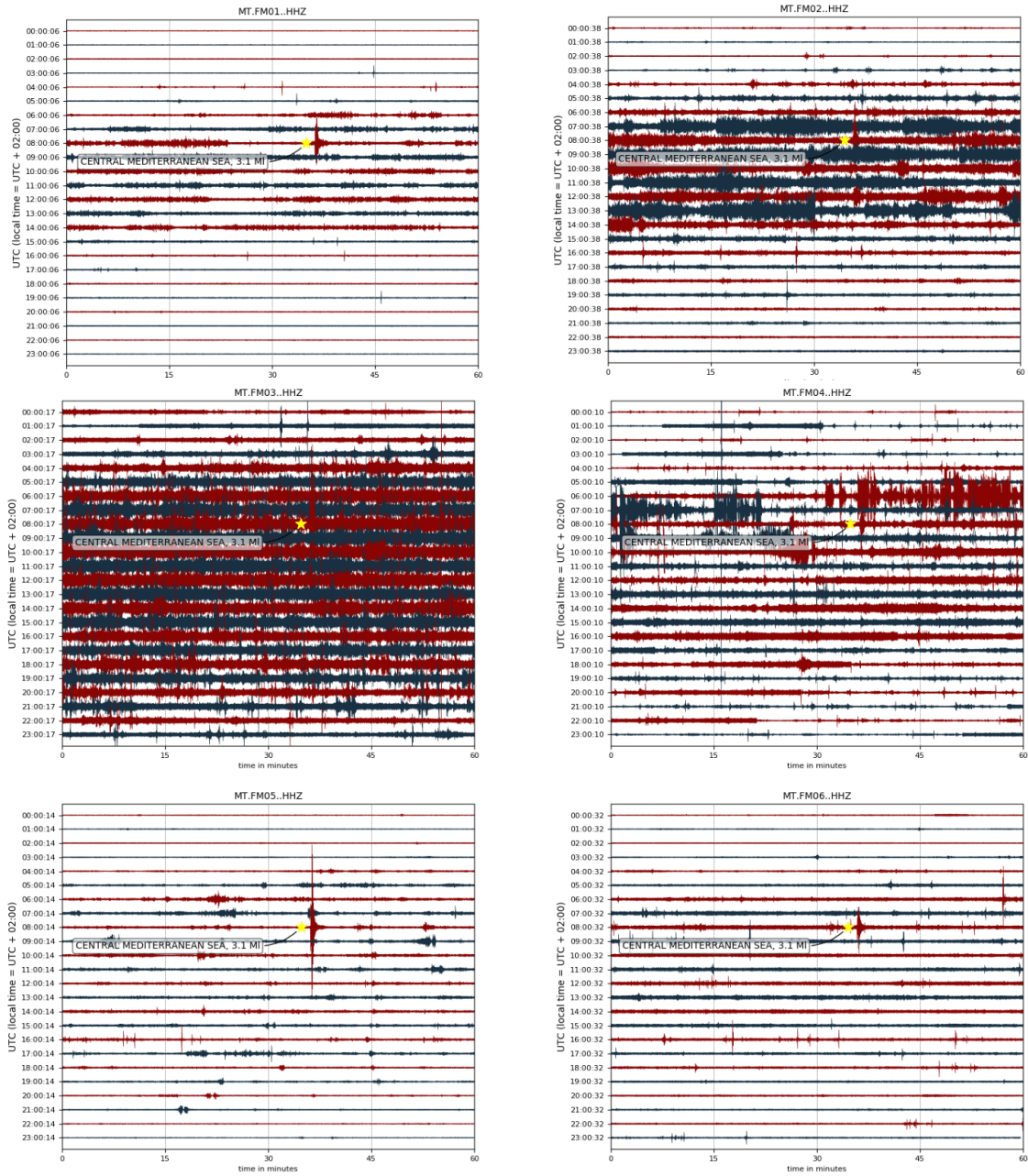


Figure 3: 24h waveform plots on the temporary network stations for the 23rd of November 2017. One of the largest offshore regional earthquakes (ML 3.1) during the study period occurred on this day, indicated with a yellow star.

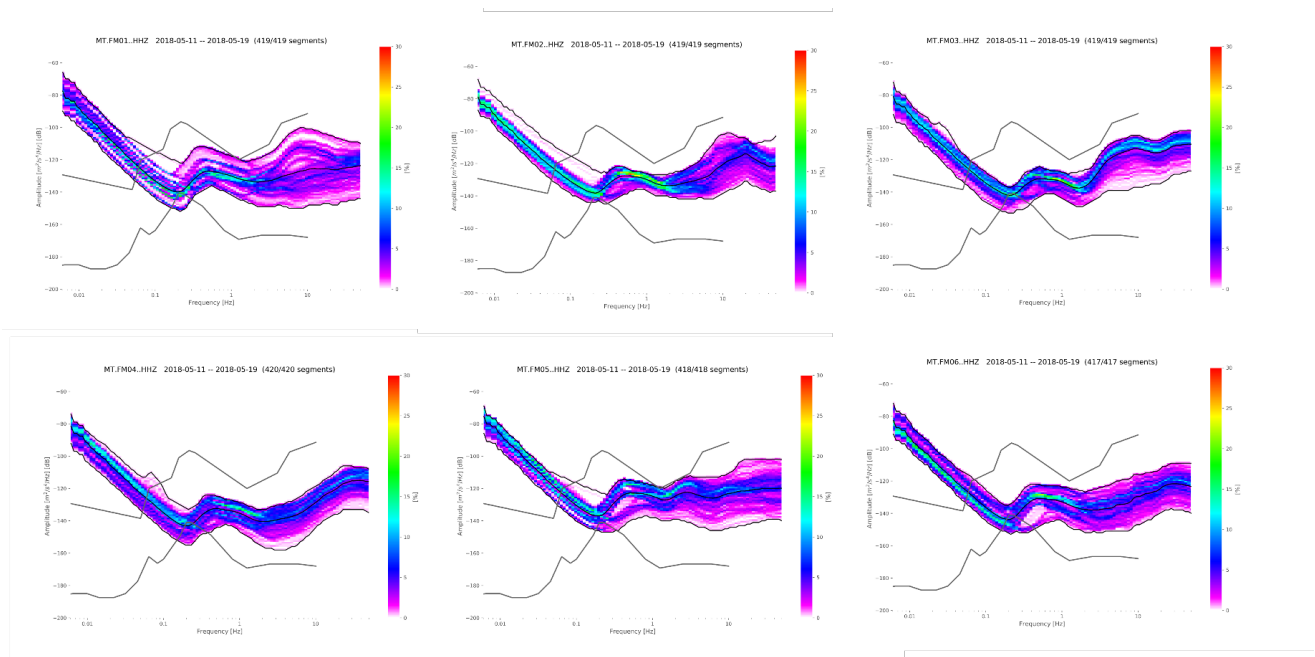


Figure 4: PPSD plots for the period 11 to the 19th of May, 2018. The PPSD plots lie within the Peterson noise limits (black curves, Peterson (1993)). Frequencies below 0.5 Hz should not be considered since the instruments were short-period stations.

mer periods (figures 10 and 11, respectively). In general, the mean PPSD curves for all stations are higher in winter than in summer, as expected. The most significant changes between the summer and the winter season are observed in stations FM01 and FM05. FM01 is probably the station most vulnerable to wave action, being close to an exposed coastline. At FM05, the mean curve in winter lies close to the NHNM in the 1 – 3 Hz frequency range. For this station, the NHNM in this frequency range is exceeded during several days, even in the summer.

To evaluate the anthropogenic effect on noise levels day and night periods are compared separately (figures 12 and 13, respectively). The 24h periods between Mondays to Thursdays are selected to avoid the noise that is created by nighttime activities during the weekends. Then the time periods 01:00 – 04:00 (night) and 16:00 – 19:00 (day) are selected as the most representative of low or high human activity. At all stations, the mean noise level is clearly higher in the daytime than at nighttime at frequencies above 1 Hz, associated with cultural/industrial noise. However, all the stations seem to remain within the noise limits.

To isolate the human activity noise, while focusing on the weather effects, the night periods of winter and summer are compared (figures 14 and 15, respectively). As expected, the summer nights are quieter, as reflected by broader curves reaching lower noise values. The stations most affected are FM02, FM03, and FM06, as at these stations, all curves drop to lower levels. As for the

rest of the stations, broader curve ranges from lower to higher noise levels are observed during summer, reflecting the calmer weather conditions. FM01 and FM05, in particular, show a much larger number of low-noise periods during the summer, as expected.

4.3 Data availability and Data loss

Figure 5 shows the data availability for the FM stations during the whole one-year period. The sheltered locations selected provided continuous data recordings with only 2 incidents of data loss. At Mdina the flash-card corrupted, causing data loss of one month (figure 5, FM03). At Bahrija (FM05), the station was unplugged by mistake during Christmas celebrations causing one-week data loss (figure 5, FM05).

4.4 Earthquake Location

We evaluate the improvement in earthquake location of the new network. Manual picking of the waveforms recorded on the enhanced network was performed for all the events that were detected using the single station location algorithm LESSLA (Agius et al., 2011). The relocation of the events were made using NonLinLoc software (Lomax et al., 2000). The initial results of the relocation are encouraging with small spatial errors, less than 1.8 km on average. The new relocated events detected from all the stations of the enhanced network for the period of June 2017 to September 2018 are shown in figure 6. The relocated events are colour coded according to their depth and scaled according to their local

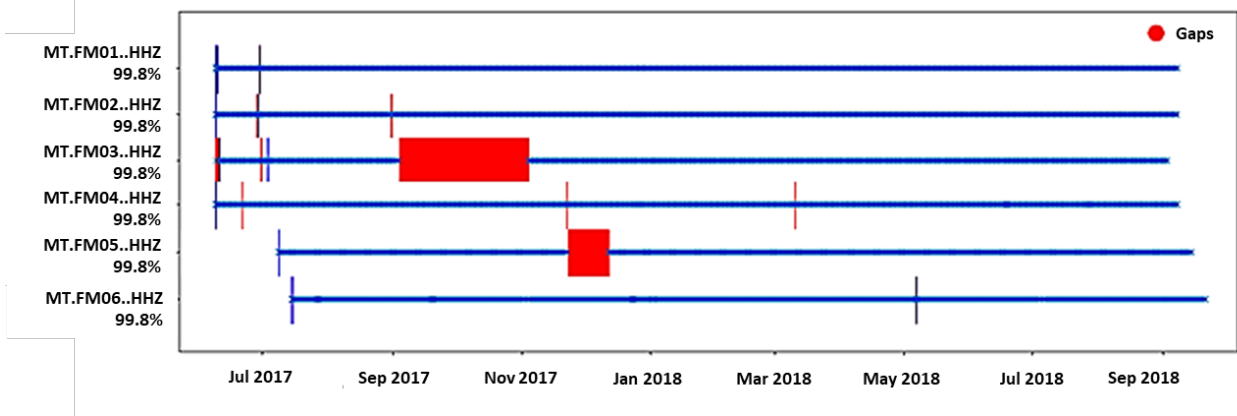


Figure 5: Data availability plot for the FM stations. Data gaps are marked with red colour.

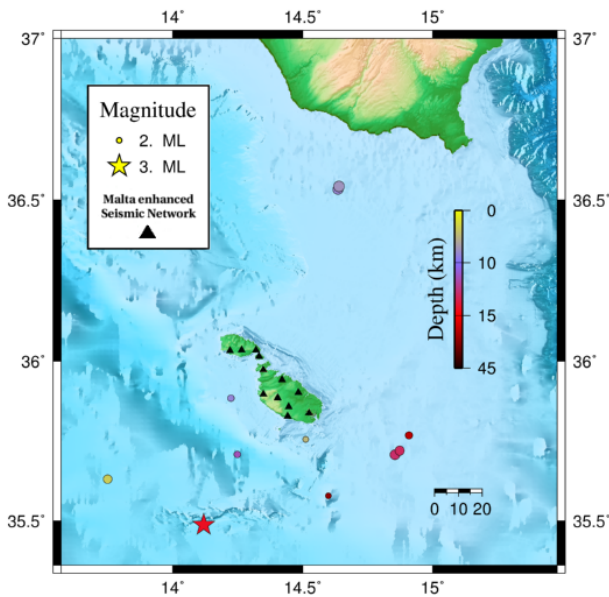


Figure 6: Examples of relocated offshore events detected on all the stations of the enhanced network during the period of June 2017 to June 2018. The ML 3.1 event that occurred on 23rd of November 2017 at around 50 km SW of Malta is marked with a red star.

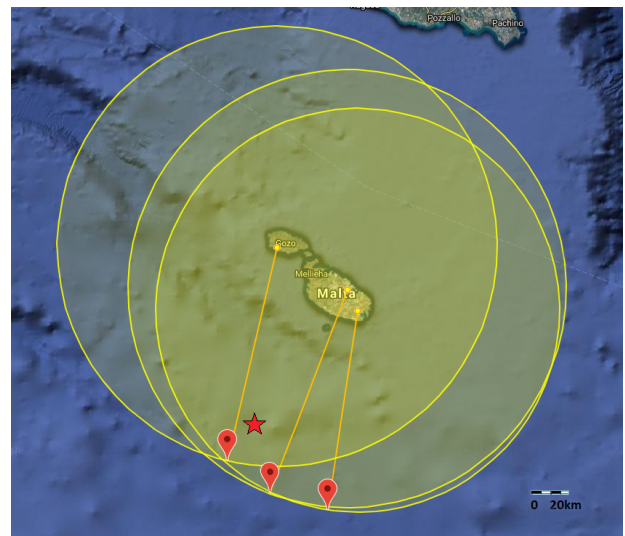


Figure 7: LESSLA solutions marked with red markers for the M_L 3.1 November event. NonLinLoc solution is marked with a red star. Besides the fact that LESSLA solutions appear to be toward the same direction, the NonLinLoc event appears to coincide with the direction of the intersection of the circles.

magnitude. The new network enables us to obtain depth estimation, with the initial depths of the events ranging from 3.5 to 12 km. Depth determination is crucial for the identification of active faults and reliable location uncertainties. On the contrary, the single station location is not able to provide depth, and the location uncertainties are empirically assigned by the analyst. As an example of improved location capability, the solution for one of the most significant offshore events during the study period (also indicated on the 24h plots of figure 3, as described above) is compared with the single station location (figure 7). The ML 3.1 event that occurred on the 23rd of November 2017, about 50 km SW of Malta (figures 6 and 7, marked with a red star), had a depth of 14.4 km, as computed by NonLinLoc. In figure 8 (bot-

tom), the waveforms of the vertical component of all the FM stations for this event are plotted. Stations FM03 and FM05 appear to have significant amplification on the waveforms due to the underlying clay layer. In spite of the noise level, a clear identification of P and S arrivals was possible. The solution gave an RMS travel time error of 0.34s, a 2.1km horizontal and 1.2km depth error. LESSLA locations for the stations XLND, MSDA, WDD for the same event differ from each other by up to 20 km (figure 7, red markers). This is partly due to the low signal-to-noise ratio at the P-arrival that introduces errors in single station location (figure 8). Although all LESSLA solutions appear to point to a relatively similar source region, the NonLinLoc event location appears to coincide with the direction of the intersection of the circles and is assumed to be the most accurate solution. The difference in the epicentral distances, between LESSLA and NonLinLoc, might also be explained by the introduction of depth to the estimation of the hypocentral depth.

5 Conclusions

To explore the potential of enhancing the ML Seismic Network, we installed six temporary, short-period stations for 15 months, as part of the FASTMIT project, getting very encouraging results. Although the Maltese islands are less than 300 km² in area, the country benefits in more than one way from having a relatively dense seismic network. Being a small island means that ambient noise from marine sources, as well as inland anthropogenic noise, makes it challenging to find seismically quiet sites. Nevertheless, the PPSD analysis of the additional network stations has shown that most stations have an acceptable noise level that is within the Peterson limits (Peterson, 1993).

In general, such an extended network will provide remarkable improvement in the detection and location of seismic and microseismic activity onshore and close to the Maltese shores. While single-station location by polarisation analysis is adequate, and may even be quite accurate, for locating regional events with a good signal-to-noise ratio at the P-arrival, the algorithm and procedure presently being used may fail for events closer than, approximately 10 km from the station. This network, or a subsequent one, will, therefore, give an unprecedented opportunity for studying the activity of local faults that are known to have generated microearthquakes in the recent past. Together with data from surrounding networks in the Central Mediterranean, it will also provide better location accuracy for more energetic events in the Sicily Channel. Moreover, the location of stations on sites overlying a thick buried clay layer will offer a unique opportunity to perform site spectral ratio analysis in which the response of such a geological

setting to earthquake shaking can be directly studied. A more detailed description of the recorded seismicity during 2017/2018 using this network, and showing the above improvement in earthquake detectability, will be the subject of a further study.

References

- Agius, M. R., D'Amico, S., Galea, P. & Panzera, F. (2014). Performance evaluation of Wied Dalam (WDD) seismic station in Malta. *Xjenza*, 2(1), 78–86.
- Agius, M. R. & Galea, P. (2011). A single-station automated earthquake location system at Wied Dalam Station, Malta. *Seismol. Res. Lett.*, 82(4), 545–559.
- Agius, M. R., Galea, P. & D'Amico, S. (2015). Setting up the Malta Seismic Network: Instrumentation, site selection and real-time monitoring.
- Beyreuther, M., Barsch, R., Krischer, L., Megies, T., Behr, Y. & Wassermann, J. (2010). Obspy: A Python toolbox for seismology. *Seismol. Res. Lett.*, 81(3), 530–533.
- Boschi, E. & Morelli, A. (1994). The MEDNET program. *Annals of Geophysics*, 37(5).
- Bragato, P. L., Costa, G., Gallo, A., Gosar, A., Horn, N., Lenhardt, W., Mucciarelli, M., Pesaresi, D., Steiner, R., Suhadolc, P., Tiberi, L., Zivcic, M. & Zoppé, G. (2014). The central and eastern european earthquake research network-CE3RN. *EGU General Assembly Conference Abstracts*, 16.
- Farrugia, D., Paolucci, E., D'Amico, S. & Galea, P. (2016). Inversion of surface wave data for subsurface shear wave velocity profiles characterized by a thick buried low-velocity layer. *Geophysical Journal International*, 206(2), 1221–1231.
- Galea, P. (2007). Seismic history of the Maltese islands and considerations on seismic risk. *Ann. Geophys.*, 50(6).
- Galea, P., Bozionelos, G., D'Amico, S., Drago, A. & Colica, E. (2018). Seismic signature of the Azure Window collapse, Gozo, Central Mediterranean. *Seismological Research Letters*, 89(3), 1108–1117.
- Lomax, A., Virieux, J., Volant, P. & Berge, C. (2000). Probabilistic earthquake location in 3D and layered models: Introduction of a Metropolis-Gibbs method and comparison with linear locations. *Thurber CH, Rabinowitz N (eds) Advances in seismic event location*, 101–134.
- McNamara, D. E. & Buland, R. P. (2004). Ambient noise levels in the continental United States. *Bull. Seismol. Soc. Am.*, 94(4), 1517–1527.
- Pedley, H. M., House, M. R. & Waugh, B. (1976). The geology of Malta and Gozo. *Proc. Geol. Ass.*, 87(3), 325–341.

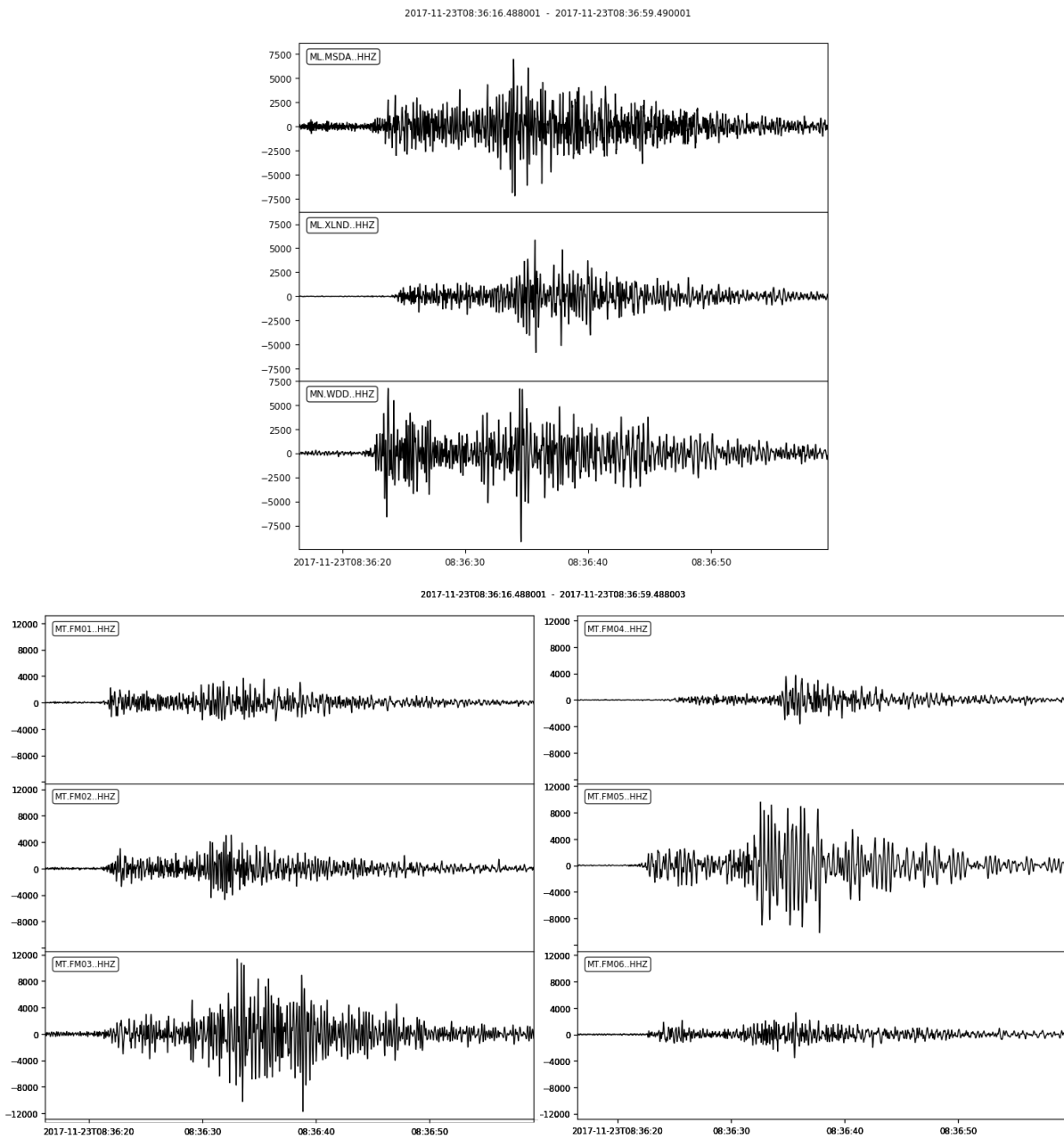


Figure 8: Top: Waveforms of the M_L 3.1 event recorded at MSN broadband stations MSDA, XLND, and WDD. In spite of the relatively good waveform quality, noise is present and makes accurate P, S phase, and back azimuth determination difficult, introducing errors in the quality of the solution. Bottom: Vertical component waveforms for the same event as it was recorded at the FM stations. (1-10Hz filter is applied on all waveforms). The S-wave amplification for stations FM03 and FM05, which lie above a buried layer of clay, is evident.

- Peterson, J. (1993). Observations and modelling of seismic background noise. *U.S. Geol. Surv. Open-File Rept.*, 93–322.
- Petricca, P. & Babeyko, A. Y. (2019). Tsunamigenic potential of crustal faults and subduction zones in the Mediterranean. *Scientific Reports*, 9(1).
- Rossi, G., Basili, R. & FASTMIT Working Group. (2016). The FASTMIT project (faglie sismogeniche e tsunamigeniche nei mari italiani).

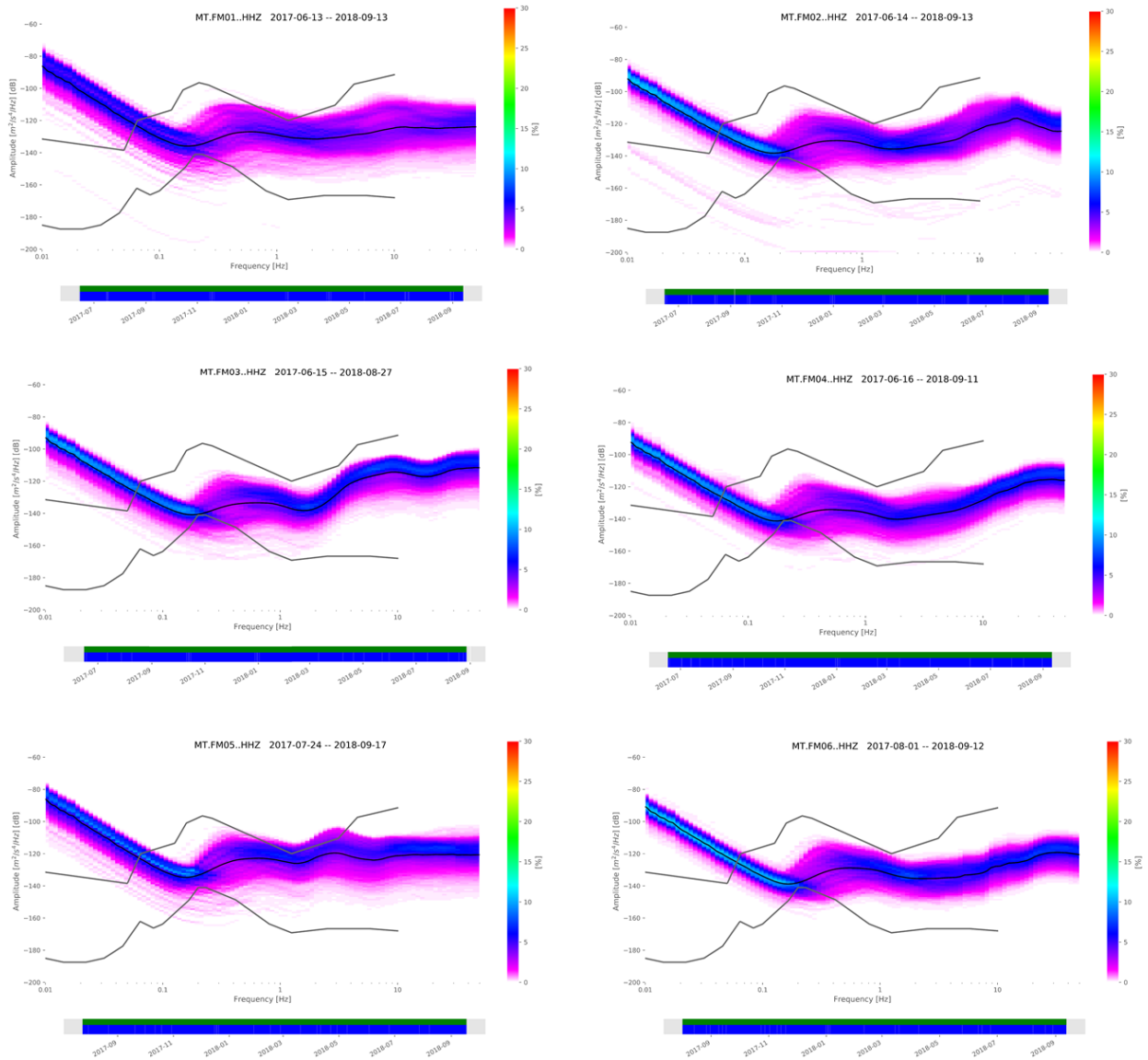


Figure 9: Probabilistic Power Spectral Density (PPSD) plots for the duration of the experiment illustrating the overall performance of each station of the FASTMIT network. The PPSDs are obtained by analyzing continuous traces of recordings cut into 1 hour windows at steps of 30 minutes. The PPSDs demonstrate the amplitudes most frequently observed at each frequency (Beyreuther et al., 2010; McNamara et al., 2004). Black curves: Typical upper and lower noise limits (Peterson, 1993), and average values of the PPSD.

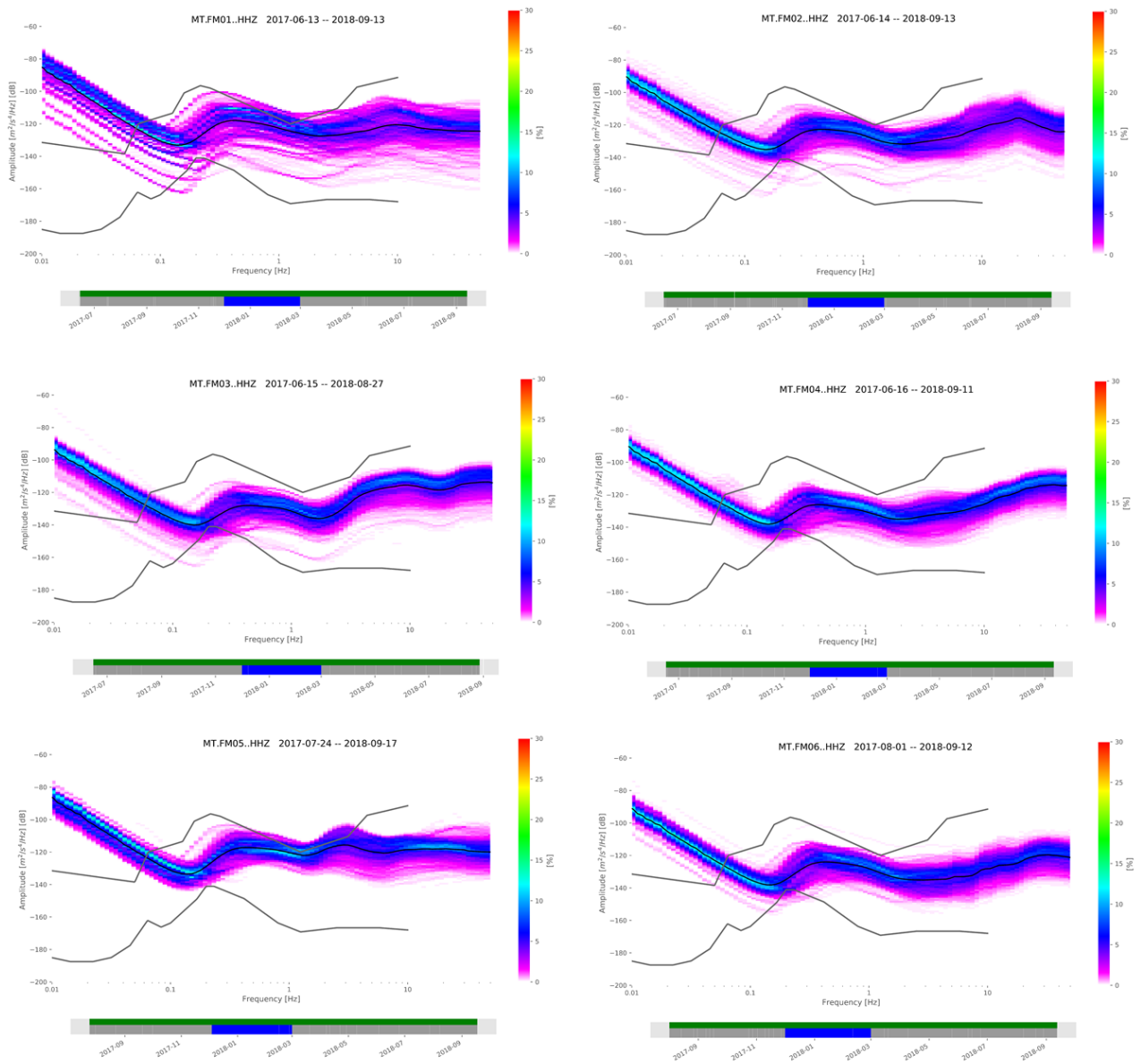


Figure 10: Same as figure 9, but for winter time period.

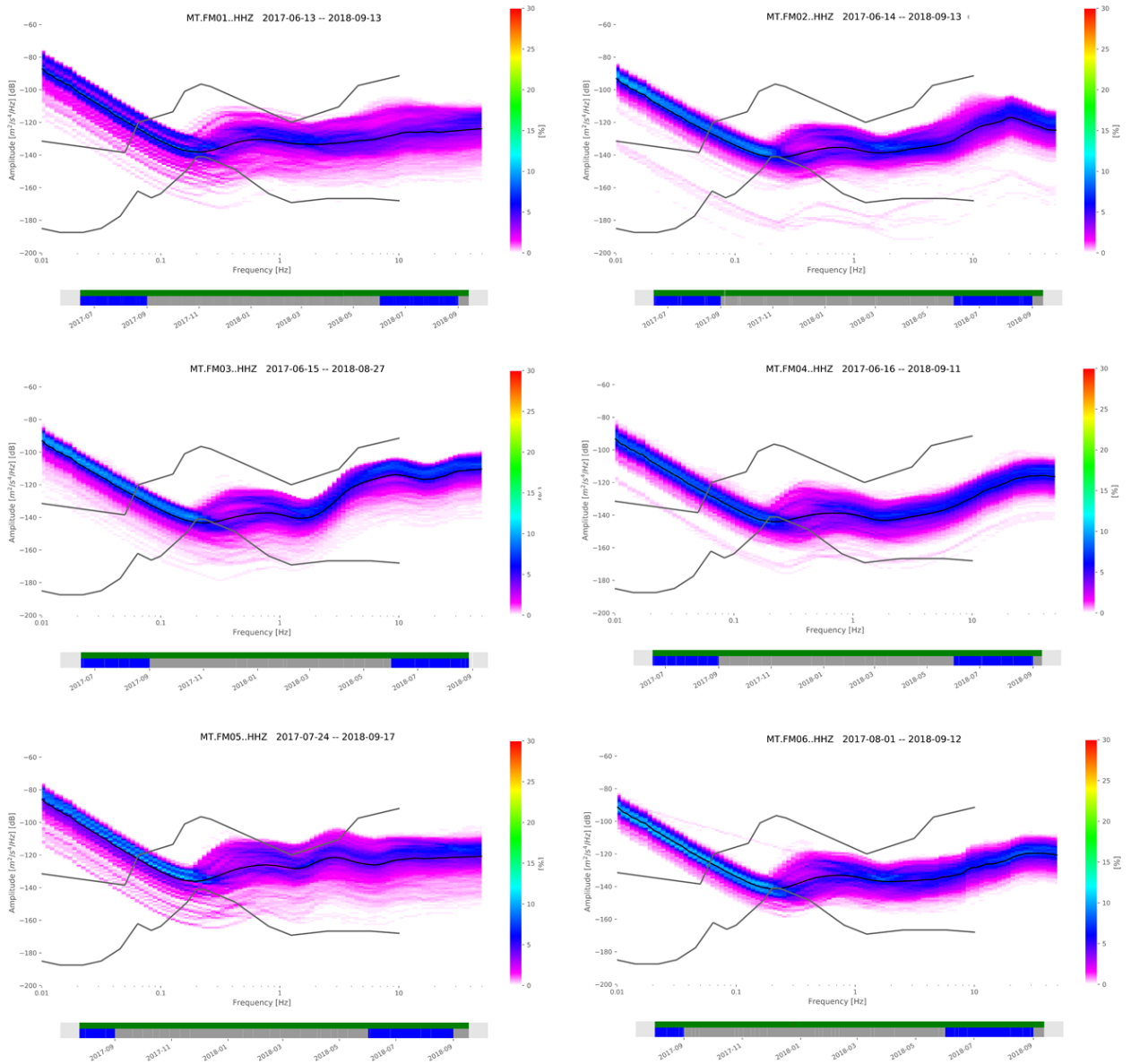


Figure 11: Same as figure 9, but for summer time period.

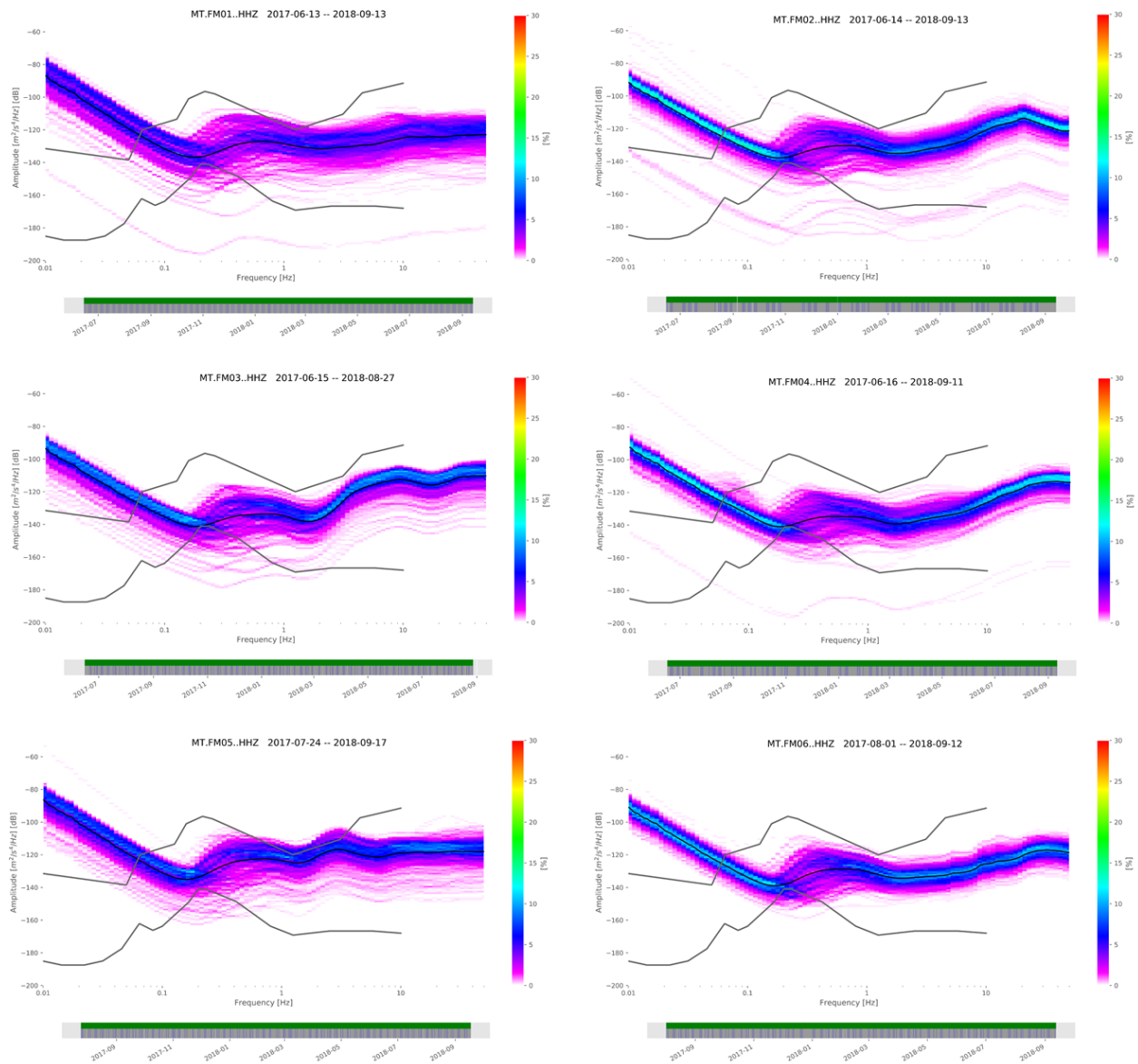


Figure 12: Same as figure 9, but for week days.

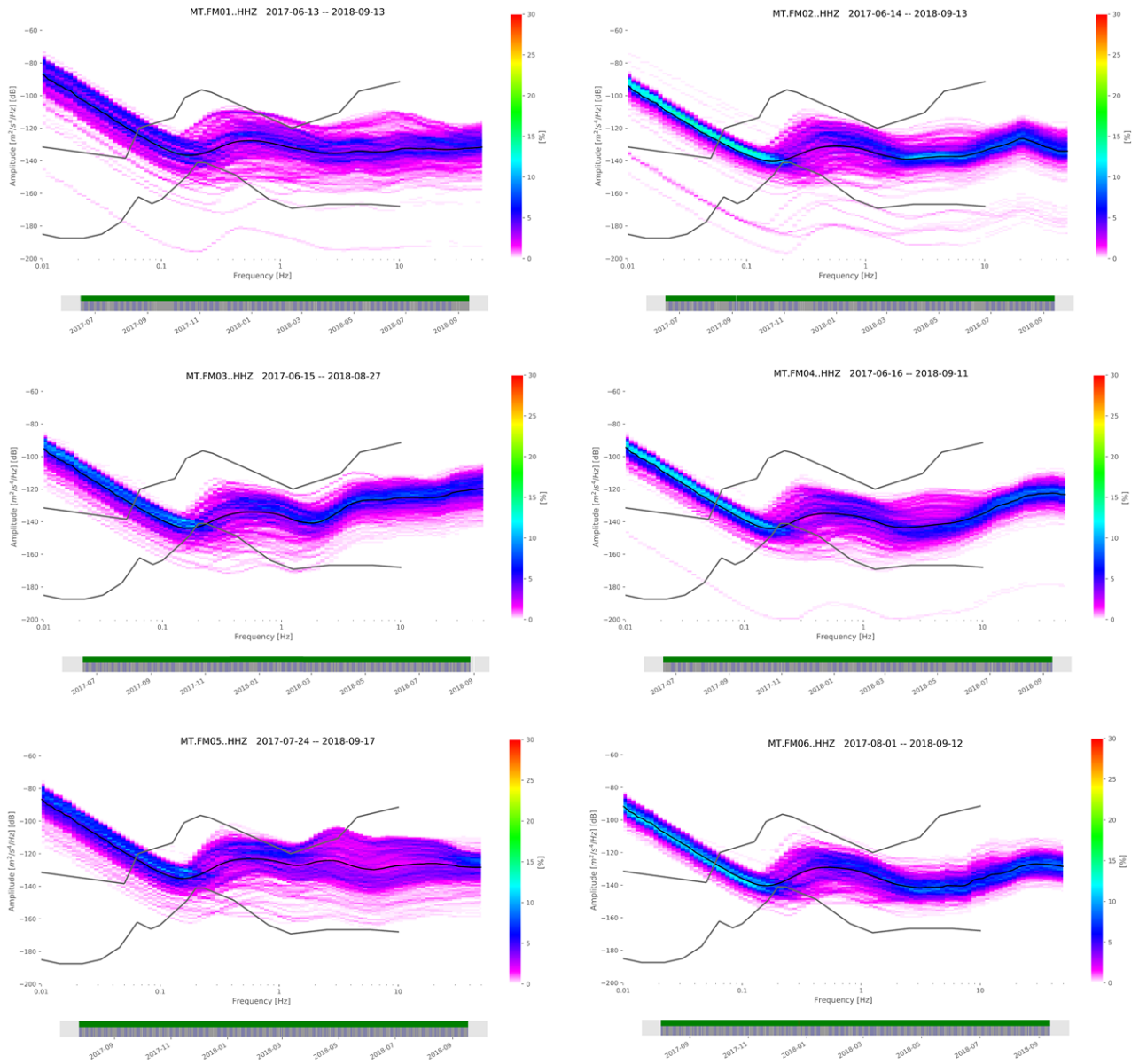


Figure 13: Same as figure 9, but for week nights.

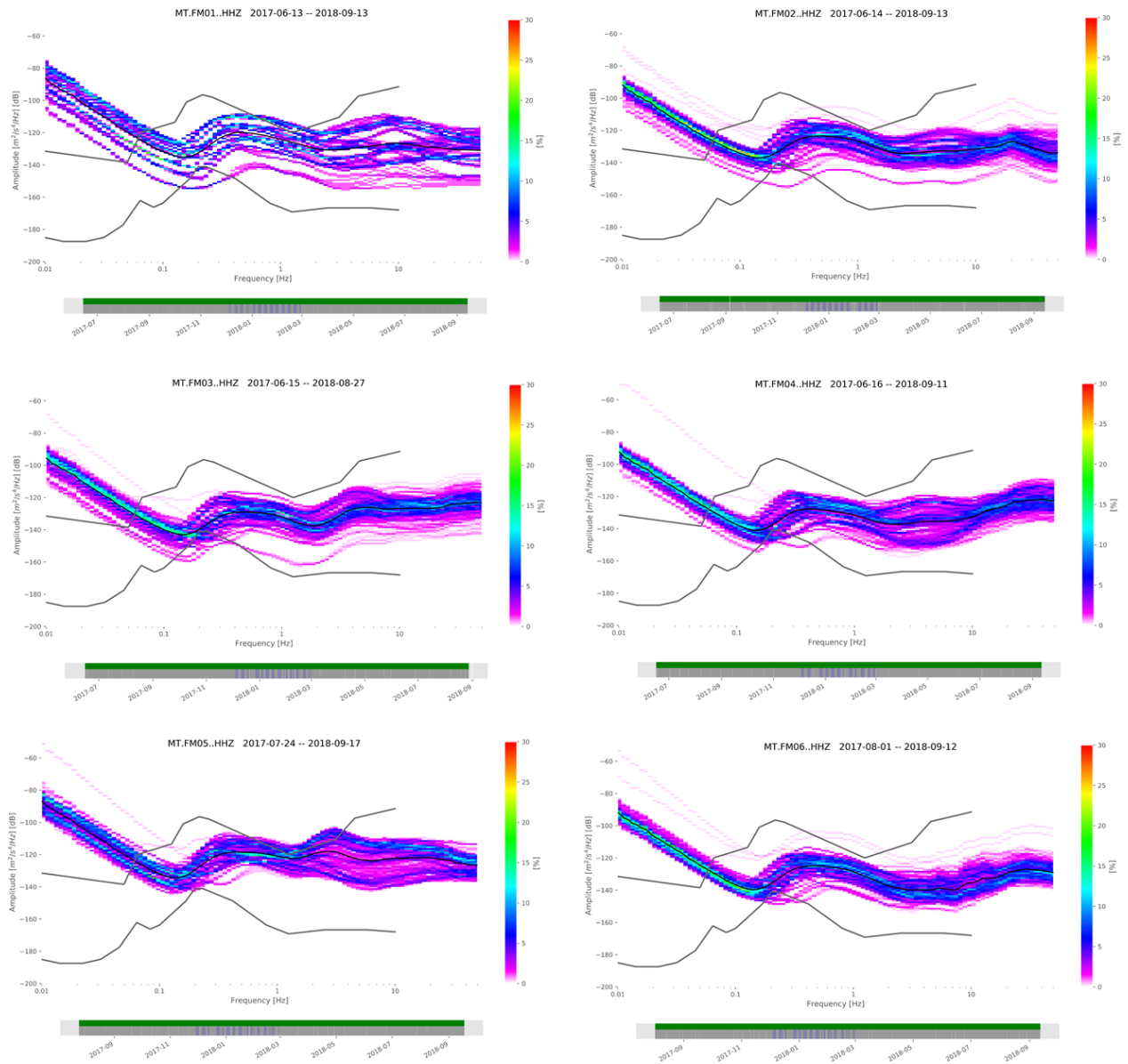


Figure 14: Same as figure 9, but for winter week nights.

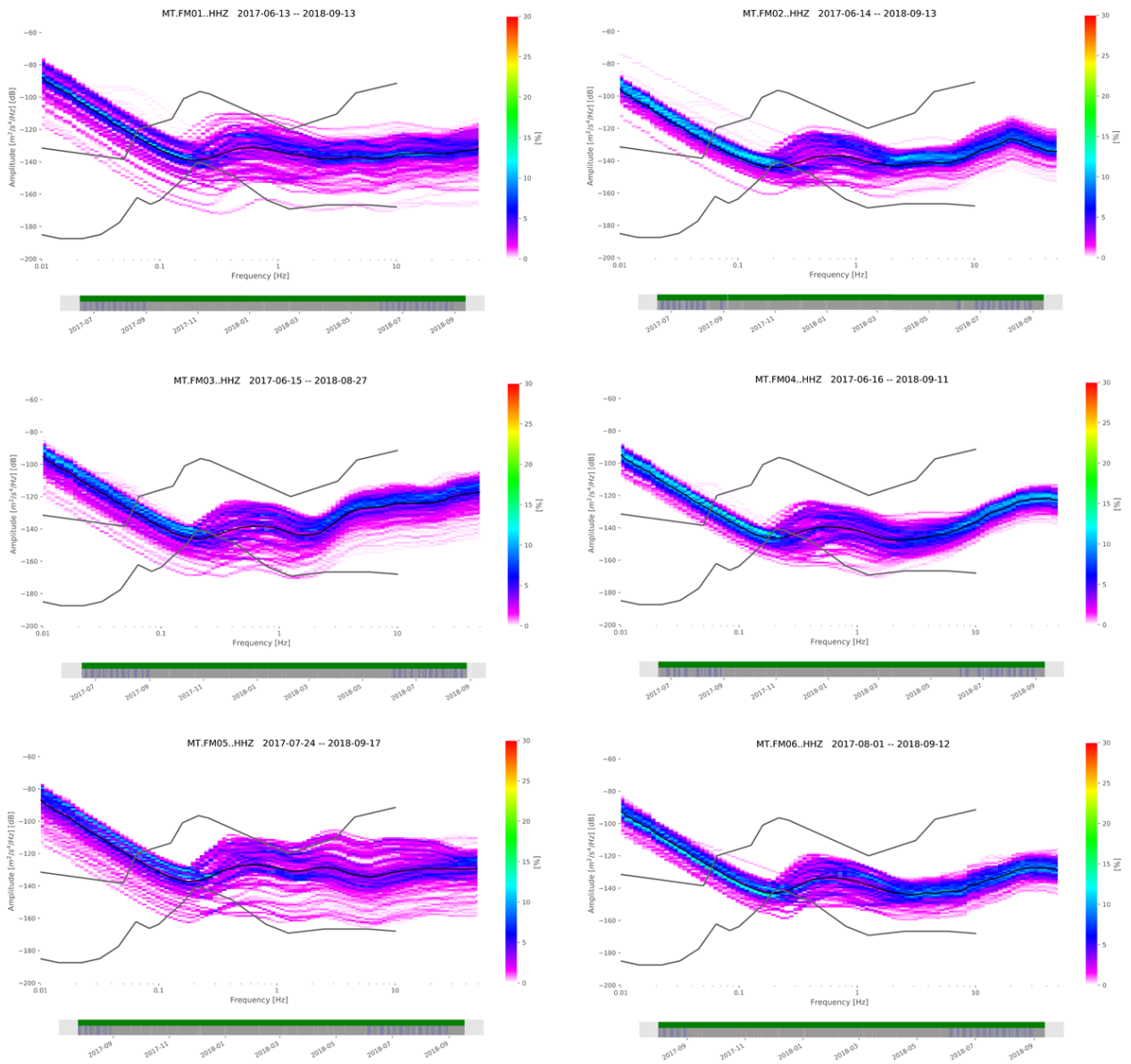


Figure 15: Same as figure 9, but for summer nights.